

Brainformer: Modeling MRI Brain Functions to Machine Vision

Xuan-Bac Nguyen¹, Xin Li², Samee U. Khan³, Khoa Luu¹

¹Department of Electrical Engineering and Computer Science, University of Arkansas, AR

²Department of Computer Science, SUNY Albany, NY

³Department of Electrical and Computer Engineering, Mississippi State University, MS

xnnguyen@uark.edu, xli48@albany.edu, skhan@ece.msstate.edu, khoaluu@uark.edu

Abstract

“Perception is reality”. Human perception plays a vital role in forming beliefs and understanding reality. Exploring how the human brain works in the visual system facilitates bridging the gap between human visual perception and computer vision models. However, neuroscientists study the brain via Neuroimaging, i.e., Functional Magnetic Resonance Imaging (fMRI), to discover the brain’s functions. These approaches face interpretation challenges where fMRI data can be complex and require expertise. Therefore, neuroscientists make inferences about cognitive processes based on patterns of brain activities, which can lead to potential misinterpretation or limited functional understanding. In this work, we first present a simple yet effective Brainformer approach, a novel Transformer-based framework, to analyze the patterns of fMRI in the human perception system from the machine learning perspective. Secondly, we introduce a novel mechanism incorporating fMRI, which represents the human brain activities, as the supervision for the machine vision model. This work also introduces a novel perspective on transferring knowledge from human perception to neural networks. Through our experiments, we demonstrated that by leveraging fMRI information, the machine vision model can achieve potential results compared to the current State-of-the-art methods in various image recognition tasks.

1. Introduction

Recent studies in machine vision understanding [14, 19, 21, 28, 34, 57] have demonstrated the effectiveness of single-encoder models through pretraining on image datasets, e.g., ImageNet [12]. These methods are designed to acquire universal visual representations of objects that can be flexibly applied to various downstream tasks, including object detection and semantic segmentation. Nonetheless, the most significant limitation of these methods lies in the costly annotation process, mainly when applied at a large scale. In

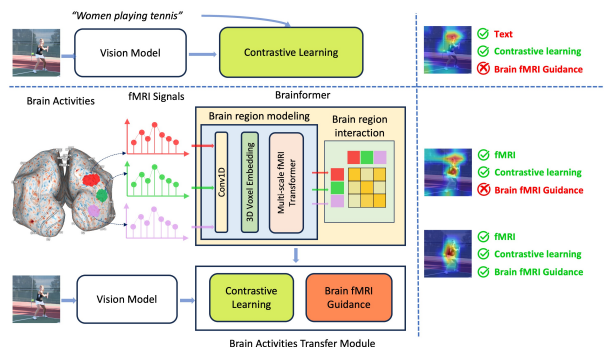


Figure 1. Given a pair of images and fMRI signals, Brainformer can explore the local patterns of fMRI signals from brain regions and discover how these regions interact with each other. **Best view in color**

response to this challenge, self-supervised techniques have emerged [4, 20, 41]. They aim to acquire visual representations without incurring human annotation expenses while delivering commendable performance compared to supervised methods.

Deep learning has recently experienced a surge in the development of foundational language models, e.g., BERT [13], GPT-2, GPT-3 [6], RoBERTa [33], T5[50], BART[29]. These models are typically trained on extensive datasets, often employing self-supervision at a large-scale web database. They have showcased their efficiency across a wide range of downstream tasks, utilizing strategies like zero-shot, few-shot, or transfer learning to extend the boundaries of large-scale modeling toward achieving human-level intelligence. Using the capabilities of text foundation models, a line of studies [23, 48, 64] has illustrated the feasibility of image-text foundation models. They encompass two encoders, i.e., an image encoder and a text encoder, jointly trained through contrastive learning. Apart from generating visual embeddings for tasks centered on vision alone, these image-text models can also generate textual embeddings that share the same latent space.

From the success of text as supervision for the visual model, we ask what had been posed in the early days of

artificial intelligence: *What if human brain behaviors can serve as the guiding force for the machine vision models?*. To answer this question, we found that Functional Magnetic Resonance Imaging (fMRI) is a neuroimaging technique that measures changes in blood flow and oxygenation in the brain, allowing researchers to observe brain activities in real-time. fMRI has provided valuable insights into various aspects of human cognition and neuroscience. For example, fMRI can help identify the specific regions of the brain that are active during various cognitive tasks. Studies have shown that different intelligence-related tasks activate specific brain areas, such as problem-solving or memory. In addition, human intelligence is not just about the activity of individual brain regions but also about how different brain regions communicate. fMRI can reveal functional connectivity patterns, highlighting networks involved in various cognitive processes.

While text typically reflects the outcomes of the recognition process, fMRI captures the dynamics of the cognitive processes involved. Consider, for instance, an examiner tasked with describing the context of an image, such as “A man is sitting on the chair.” Initially, they focus on the man and then shift attention to the chair, determining the interactions between these objects, specifically, the act of sitting. Subsequently, they conclude the context in the text form. When encountering this description for the first time, it remains unclear which object the examiner attended to first or whether other smaller objects influenced their perception. Notably, **this information can be encoded in fMRI signals**. By analyzing specific brain regions or regions of interest, we can explore the whole recognition process of the human brain. This work provides a promising approach to further studies and endeavors to bridge the gap between human intelligence and deep neural networks. The contributions of this work can be summarized as follows.

Contributions of this Work: This paper presents a novel Transformer-based framework, named Brainformer, to analyze and leverage fMRI signals as human brain activities to supervise the machine vision learning model. We present a simple yet effective way to encode fMRI features. Then, a novel *Brain 3D Voxel Embedding* approach is introduced to preserve spatial signal information. The proposed Brainformer explores the patterns within specific regions of interest in the human brain that signify the human *attention process* via the Multi-scale fMRI Transformer module. It can learn the correlation between these regions, helping to mimic the human *recognition process*. By incorporating these capabilities, Brainformer reveals mechanisms in the human recognition system. Second, a new Brain fMRI Guidance Loss function is presented to distill information from fMRI extracted using Brainformer. It serves as a guidance signal to enhance the performance capabilities of vision models. Finally, Brainformer is designed for self-

supervised learning and trained as an end-to-end deep network. It consistently outperforms previous State-of-the-Art Self-supervised learning methods across standard benchmarks, i.e., object detection, instance segmentation, semantic segmentation, and brain response prediction.

2. Related Work

Vision Pretraining. Pretraining on the large-scale dataset such as ImageNet [12], Instagram [39], or JFT [65] has become a popular approach for many visual recognition problems, e.g., classification, localization, or segmentation, etc. Despite this method has great success, it is limited by the number of annotated training data that is costly to collect. Recently, self-supervised training has been proposed to address this problem. For example, BEiT [4] inspired by BERT [13] in natural language processing to make a masked image model. Similarly, SimMIM [62] and MAE are proposed to randomly remove the image patches and then use the encoder-decoder model to regress the masked pixel values. Nonetheless, these methods use the vision modality as the only input and are unsuitable for tasks involving images and text.

Vision-Language Pretraining. Significant advancements have occurred in vision-language pertaining [23, 30, 38, 45, 49, 58–60, 63, 66, 67]. This approach aims to encode both visual and text information into a model. Initial work, e.g., LXMERT [55], UNITER [9], and VinVL [68], depended on pre-trained object detection modules like Fast(er) R-CNN [51] to extract visual representations of objects. Subsequent studies, such as ViLT [27] and VLMo [5], tried to integrate vision and language transformers and then train a multimodal transformer from scratch. Recent work has proposed Image-Text foundation models that bridge the gap between image and text understanding. It is worth mentioning that CLIP [48] and ALIGN [22] leverage dual-encoder architecture pre-trained on noise image-text pairs using contrastive learning. It has achieved robust image and text representation, suitable for cross-model alignment tasks and zero-shot image classification. Another line of research [46, 58, 60] explores encoder-decoder models trained with generative losses, showcasing impressive performance in vision-language benchmarks while maintaining strong visual encoder capabilities for classification tasks.

Decoding functional MRI. Decoding visual information from fMRI signals has been studied for a decade [11, 17, 18, 24, 56]. Most of these studies aimed to explore the hidden information inside the brain. It is a difficult task because of the low signal-to-noise ratio. Recently, with the help of deep learning, the authors in [10, 31, 43, 44, 52, 54] proposed methods to reconstruct what humans see from fMRI signal using diffusion models. There are limited works [40, 42] that incorporate human brain activities for transfer learning. However, these methods still need to be improved

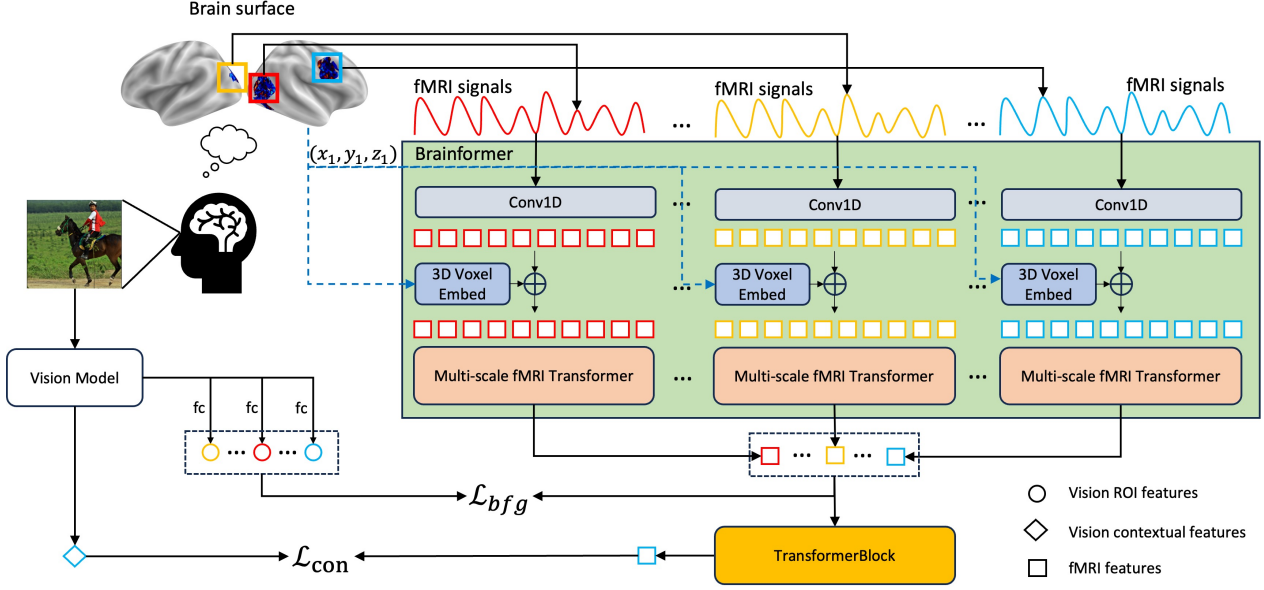


Figure 2. Brainformer utilizes fMRI signals from specific brain regions as input, extracting the local features representing patterns within each region. The TransformerBlock measures the correlation among these regions to emulate brain activities. This information is subsequently transferred to the vision model through Contrastive Loss and Brain fMRI Guidance Loss.

in exploring the working mechanism of the human brain.

3. The Proposed Approach

3.1. Motivations

Different from recent studies on decoding fMRI [10, 52, 54], our goal is not only to explore valuable vision information from fMRI signal, i.e., semantic and structure information but also utilize them as supervision for helping to enhance the recognition capability of the vision model, a novel approach that standouts our work from previous efforts in the field. Although our approach also aims to extract feature representations of fMRI data, these previous methods still have limitations and do not apply to our problem. Firstly, prior approaches, such as those by Yu et al. [54] and Paul et al., [52] relied on linear models and MLP layers to generate fMRI feature representations. This approach cannot capture the local pattern of the signals, especially the non-linear or complicated patterns. Kim et al. [26] presented SwiFT for self-training fMRI in 4D data, which does not apply to our problem. On the other hand, MindVis [10] utilized a Masked Brain Model inspired by MAE, which explored local patterns but ignored the correlations between multiple voxels, which describes how neurons interact inside the brain. Furthermore, MindVis failed to leverage the 3D spatial information in fMRI signals, which is crucial in understanding the relationships between voxels. Most notably, none of these approaches leverage characteristics of functional regions of interest (ROI) within the brain, which contain rich information about visual stimuli.

The fMRI contains a structured and semantically rich representation of information since fMRI captures brain activities in the context of a person engaging in visual tasks. It provides ground truth data about how the human brain responds to visual stimuli. According to recent studies [15, 25, 47], the brain can be divided into several Regions of Interest (ROI), where each region holds a different function. Especially in the scope of visual cognition, these are 6 regions specified as Early retinotopic visual regions (*prf-visualrois*), Body-selective regions (*floc-bodies*), Face-selective regions (*floc-faces*), Place-selective regions (*floc-places*), Word-selective regions (*floc-words*) and Anatomical streams (*streams*). In summary, these regions are responses for processing information related to the human body, face, place, motion, or objects regarding identification, recognition, etc. Therefore, the fMRI signals from these regions can be used to train computer vision models, providing a reference for what the brain is “seeing” during the training. By training vision models jointly with brain activities observed in fMRI scans, they can explore the relationship between the visual information processed by the brain and the visual information that models are learning. It can help uncover how the brain represents and processes visual information.

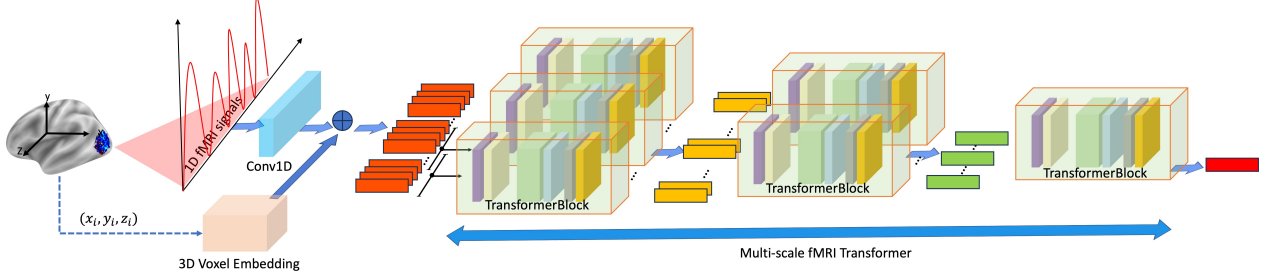


Figure 3. The details of Multi-scale fMRI Transformer module.

3.2. Brainformer

As aforementioned, human intelligence is presented by the activity of individual brain regions of interest and how they interact with each other. Inspired by this concept, we introduce Brainformer, as shown in Figure 2, a model that takes fMRI signals from Regions of Interest in the brain as inputs. The proposed model comprises two primary modules. First, we introduce a Mutli-scale fMRI Transformer, as shown in Figure 3, designed to uncover local patterns of brain activities within each ROI. Subsequently, we feed a sequence of ROI features derived from the output of the Mutli-scale fMRI Transformer into a conventional Transformer to estimate the correlation and interaction among multiple ROIs. In the following sections, we focus on the design of the Mutli-scale fMRI Transformer, as detailed in Section 3.2.3. Section 3.2.4 introduces brain cognitive features which represent for correlation between brain regions. Prior to that, we present an efficient way to extract features of raw signals in Section 3.2.1. Additionally, we introduce a novel technique called Brain 3D Voxel Embedding in Section 3.2.2, aimed to preserve the spatial information of the signals.

3.2.1 High-dimensional fMRI Feature Encoding

Let m^k be the fMRI signals of the k^{th} region of interest in the brain. This signal can be constructed using Eqn. (1).

$$m^k = [\delta(x_i, y_i, z_i)]_{i=0}^{N^k-1} \quad (1)$$

where δ is the function that takes the value of change in blood and oxygenation in the voxel coordinated at (x_i, y_i, z_i) . N^k is the number of voxels in this region. This definition shows that fMRI is a 1D high-dimension signal due to the significant value of N^k , e.g., $N^k \approx 20K$. A straightforward approach to model this signal is adopting linear or fully connected layers [52] and extracting its latent embedding. This approach, however, has two drawbacks. First, fully connected layers with high dimensional features are inefficient as it is challenging to learn useful information from the input space while maintaining a high memory usage of the model. Second, it focuses more on the global structure while ignoring the local patterns presented in the fMRI signal. To solve these two problems,

we propose Conv1D to extract features of the fMRI signal. Formally, the embedding feature of fMRI is represented in Eqn. (2).

$$\mathbf{r}^k = \text{Conv1D}(m^k) \in \mathbb{R}^{N^k \times d_r} \quad (2)$$

The \mathbf{r}^k is the embedding features of m^k after the convolution step, and d_r is the embedding dimension.

3.2.2 Brain 3D Voxel Embedding

As shown in Eqn (1), the fMRI signal is a compressed representation of Magnetic Resonance Imaging (MRI) containing detailed 3D information. However, direct learning from the flattened signal will *ignore the spatial structure*. Figure 4 illustrates this problem. Consider two voxels, denoted as $v_1 = (x_1, y_1, z_1)$ and $v_2 = (x_2, y_2, z_2)$, which are closely situated in the 3D space of MRI, but in fMRI signals representation, they appear distant from each other. Therefore, it becomes crucial to incorporate spatial information for the model to uncover deeper structural features. Meanwhile, prior studies [10, 52, 54] still need to address this problem. In light of this concept, we introduce a new approach named *Brain 3D Voxel Embedding* to capture the spatial architecture of fMRI more effectively.

Let m_i^k be the voxel in the signal m^k and (x_i^k, y_i^k, z_i^k) are the 3D coordinates of this voxel. We use Linear function to map these (x_i^k, y_i^k, z_i^k) coordinates into the same dimension, i.e., d_r dimension, as the fMRI embedding features in Eqn. (2)

$$v_i^k = \text{Linear}(x_i^k, y_i^k, z_i^k) \in \mathbb{R}^{d_r} \quad (3)$$

$$v(m^k) = \text{concat} [v_0^k, v_1^k, \dots, v_{N^k-1}^k] \in \mathbb{R}^{N^k \times d_r}$$

where v_i^k is the brain 3D voxel embedding of single voxel i^{th} , $v(m^k)$ is the embedding of the entire signal m^k . Incorporating with *Brain 3D Voxel Embedding* to the Eqn. (2), we get the features of fMRI as shown in Eqn. (4).

$$\mathbf{r}^k = \text{Conv1D}(m^k) + v(m^k) \quad (4)$$

3.2.3 Mutli-scale fMRI Transformer

While extremely powerful for a wide range of natural language processing tasks, Transformers have limitations

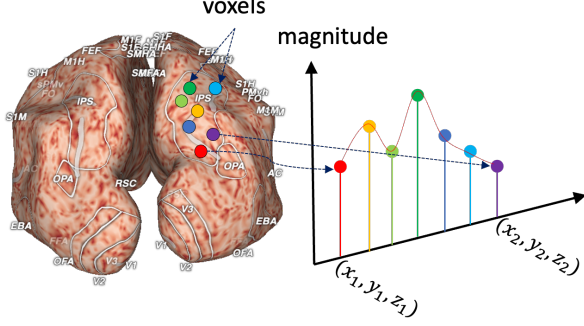


Figure 4. Two voxels, denoted $v_1 = (x_1, y_1, z_1)$ and $v_2 = (x_2, y_2, z_2)$ that are located closely in the 3D space of MRI, but in the fMRI signals, they are far away from each other.

when handling long sequences. These limitations are primarily due to the quadratic complexity of the self-attention mechanism and the model’s parameter count. In addition, the attention score might collapse and close to zero if the sequence length is considerable. Hence, using the typical transformer for lengthy fMRI signals is not a complete solution.

To deal with the long sequence in our problem, we propose the Mutli-scale fMRI Transformer, shown in Figure 3. It contains multiple levels, each level consisting of a Transformer block denoted as TransBlock. The length of the signal is reduced when passing through each level of the network until it is sufficient enough. The details of the Multi-scale fMRI Transformer are presented in Algorithm 1. In particular, each level consists of two steps:

- We first employ a slicing window with w of width that traverses the entire signal \mathbf{r}^k from its beginning to the end, with a step size of s . This process decomposes \mathbf{r}^k into smaller sub-sequences, denoted as $\mathbf{q}_i^k = \mathbf{r}^k[i*s : i*s + w]$ $0 \leq i \leq n_s = \frac{N^k}{s}$ which has a computation-efficiency length for the Transformer. The adjacent subsequences overlap by a distance of s , preventing the loss of local information, and n_s is the number of subsequences.
- We fed \mathbf{q}_i^k into the TransBlock to learn the patterns inside the signal and get the features $\bar{\mathbf{q}}_i^k = \text{TransBlock}^k(\mathbf{q}_i^k)$. After that, all the features $\bar{\mathbf{q}}_i^k$ of subsequences are gathered to form a new sequence $\mathbf{t} = [\bar{\mathbf{q}}_i^k]_{i=0}^{n_s-1}$ and then passed into the next level.

3.2.4 Brain Cognitive Features

Let $[\bar{\mathbf{q}}^k]_{k=0}^{N_r}$ be the list of fMRI features that are the outputs from the Mutli-scale fMRI Transformer. N_r is the number of regions in the brain. In particular, we define $N_r = 6$ as discussed in the section 3.1. To learn the correlation between the ROIs, we adopt another feature embedding process by feeding $[\bar{\mathbf{q}}^k]_{k=0}^{N_r}$ into a final TransBlock and receiving the brain cognitive features, denoted as $\mathbf{q} =$

$\text{TransBlock}([\bar{\mathbf{q}}^k]_{k=0}^{N_r})$.

3.3. Training Objectives

Our framework is trained by a combination of Contrastive Loss, \mathcal{L}_{con} , and Brain fMRI Guidance Loss, \mathcal{L}_{bfg} , bellow:

$$\mathcal{L} = \lambda_{con}\mathcal{L}_{con} + \lambda_{bfg}\mathcal{L}_{bfg} \quad (5)$$

where λ_{con} and λ_{bfg} are the weights of the loss functions. In this paper, we select $\lambda_{con} = \lambda_{bfg} = 0.5$. The details of \mathcal{L}_{con} and \mathcal{L}_{bfg} are described in the sections below.

3.3.1 Contrastive Loss

Let $\mathbf{p} \in \mathbb{R}^{d_r}$ be the image features extracted by the image encoder, e.g., SwinTransformer, ConvNext. We employ contrastive loss [8] to align visual representation with the brain cognitive features \mathbf{q} as in Eqn. (6).

$$\begin{aligned} \mathcal{L}_{con} = & -\frac{1}{N} \sum_i \log \frac{\exp(\mathbf{p}_i \otimes \mathbf{q}_i / \sigma)}{\sum_j \exp(\mathbf{p}_i \otimes \mathbf{q}_j / \sigma)} \\ & - \frac{1}{N} \sum_i \log \frac{\exp(\mathbf{q}_i \otimes \mathbf{p}_i / \sigma)}{\sum_j \exp(\mathbf{q}_i \otimes \mathbf{p}_j / \sigma)} \end{aligned} \quad (6)$$

where σ is the learnable temperature factor, N is the number of samples, and \otimes is the dot product.

3.3.2 Brain fMRI Guidance Loss

Besides the contrastive loss that aligns the *global context* of brain signals and stimuli image, the Brain fMRI Guidance Loss aims to align the *local context*. Since the ROI features $\bar{\mathbf{q}}^k$ is extracted from a particular region of the brain, e.g., floc-bodies, floc-faces, etc., it embeds the information on how the brain perceives the objects inside the image. If we can leverage these features as the guidance during training, the vision model can mimic the perception system of the human.

Let $\bar{\mathbf{p}}^k$ be the vision features representing a specific local context within the image, e.g., objects, persons, the background, or locations. These features can be achieved by passing pooling features of the vision model to the linear layer and then projected to the same dimension space as $\bar{\mathbf{q}}^k$. Our goal is to encourage the visual perceptions of the vision model to be similar to the ROI features of the brain. This requires maximizing the similarity between two features, $\bar{\mathbf{p}}^k$ and $\bar{\mathbf{q}}^k$. Furthermore, it is important to emphasize that the brain’s ROIs have distinct functions. Consequently, we must ensure the dissimilarity of $\bar{\mathbf{q}}^k$ with respect to all $\bar{\mathbf{q}}^g$, where $k \neq g$. To facilitate the two constraints, we propose the Brain fMRI Guidance Loss as in Figure 5 and in Eqn. (7).

$$\mathcal{L}_{bfg} = -\frac{1}{N} \sum_i \sum_k \log \frac{\exp(\bar{\mathbf{p}}_i^k \otimes \bar{\mathbf{q}}_i^k)}{\sum_g \exp(\bar{\mathbf{p}}_i^k \otimes \bar{\mathbf{q}}_i^g)} \quad (7)$$

Algorithm 1 Mutli-scale fMRI Transformer

```

1: Input: The feature  $\mathbf{r}^k$  of  $k^{th}$  fMRI signals, window size  $w$ ,
   stride:  $s$ , number of level  $h$ .
2: Output: The fMRI features  $\bar{\mathbf{q}}^k$ 
3:  $\mathbf{x} \leftarrow \mathbf{r}^k$ 
4: for  $j = 1, \dots, h$  do
5:    $\mathbf{t} \leftarrow$  empty list  $\triangleright$  Store features of subsequences
6:    $L \leftarrow |\mathbf{x}|$ 
7:   for  $i = 0, \dots, \frac{L}{s}$  do
8:      $\mathbf{q}_i^k \leftarrow \mathbf{x}[i*s : i*s + w]$   $\triangleright$  Getting subsequences
9:      $\bar{\mathbf{q}}_i^k \leftarrow \text{TransBlock}_j^k(\mathbf{q}_i^k)$ 
10:     $\mathbf{t} \leftarrow [\mathbf{t}, \bar{\mathbf{q}}_i^k]$   $\triangleright$  Gather features of the subsequence
11:  end for
12:   $\mathbf{x} \leftarrow \mathbf{t}$ 
13: end for
14:  $\bar{\mathbf{q}}^k \leftarrow \text{TransBlock}(\mathbf{x})$ 
15: return  $\bar{\mathbf{q}}^k$ 

```

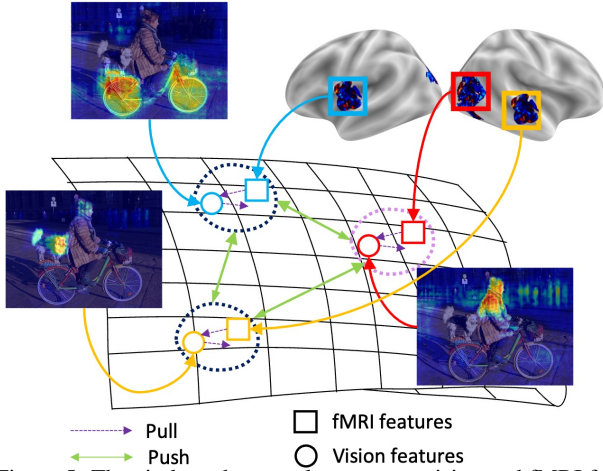


Figure 5. The circle and rectangle represent vision and fMRI features, respectively. Each color indicates a different object of interest that the human brain is processing. The Brain fMRI Guidance Loss aims to align visual and fMRI features of the same object while discriminating with features of other objects.

4. Experimental Results

4.1. Datasets

To pretrain Brainformer, we leverage the Natural Scenes Dataset (NSD) [1], a comprehensive compilation of responses from eight subjects obtained through high-quality 7T fMRI scans. Each subject was exposed to approximately 73,000 natural scenes, forming the basis for constructing visual brain encoding models. The fMRI responses of each image encompass the left hemisphere (LH) and right hemisphere (RH), with 19,004 and 20,544 voxels, respectively.

4.2. Brainformer Training

We use data from seven subjects in NSD for training and leave one for testing. The images are resized to 224×224

before feeding into the vision model. We do not use any augmentations for the image because the fMRI signals depend on the input image. Any change in vision stimuli will affect human recognition. For the fMRI signals, we divide them into six regions of interest following [16] and feed them into Brainformer simultaneously. Experimentally, we select `Conv1D` with kernel size and stride are 32 and 16, respectively. The Multi-scale fMRI Transformer is designed with a window size as $w = 64$, stride as $s = 32$, and number of levels as $h = 2$. Feature dimensions of image and fMRI signals are projected into $d_r = 768$ space. For the vision model, we select Swin-S [34] and ConvNext-S [35] as the image backbone. Brainformer is easily implemented in the Pytorch framework and trained on A100 GPUs. The initial learning rate is 0.0001 and decreases gradually following the CosineLinear policy [36]. A batch size of 64 per GPU is employed. Optimization is performed using AdamW [37] with 100 epochs, with the entire training process concluding within a few hours. The pre-trained models are used for further downstream tasks, including COCO object detection [32] and ADE20K semantic segmentation [69].

4.3. Object Detection on COCO

Settings. We conducted object detection and instance segmentation experiments using the COCO 2017 dataset, which comprises 118,000 training images, 5,000 validation images, and 20,000 test-dev images. Notably, we excluded images from the NSD dataset to prevent any data leakage, a subset of COCO. For these experiments, we utilized the MaskRCNN framework [3] implemented with mmdetect [7] for enhanced performance efficiency.

Performance. The object detection and instance segmentation results are presented in Table 1. In summary, our approach, which leverages fMRI signals for training, consistently outperforms the CLIP framework, where models rely solely on textual supervision. Specifically, when comparing Swin-S/CLIP to Swin-S/Random, the Swin-S/CLIP achieves approximately a 0.6% improvement in box/AP and a 0.8% improvement in seg/AP. However, our method Swin-S/Brainformer presents even better performance, surpassing Swin-S/CLIP by approximately 1.7% and 3.9% in object detection and instance segmentation, respectively, translating to a substantial 2.3% and 4.7% improvement compared to the same model Swin-S/Random without any pretraining method. We also observe the same results with the ConvNext-S backbone, where Brainformer achieves around 2.3% and 3.2% higher than CLIP in box/AP and seg/AP.

4.4. Semantic Segmentation on ADE20K

Settings. For semantic segmentation, we conducted training using UpperNet [61] on the ADE20K database, which includes a wide spectrum of 150 semantic categories. This dataset comprises 25,000 images, with 20,000 allocated for

training, 2,000 for validation, and 3,000 for testing.

Performance. Table 2 presents the semantic segmentation results. From these results, Swin-S/Brainformer is 1.48% mIoU (41.77 v.s 40.29) higher than Swin-S/CLIP while ConvNext-S/Brainformer maintains the performance better than ConvNext-S/CLIP by 1.65% mIoU.

4.5. Human Brain Response Prediction NSD

Settings. This experiment aims to predict the human brain response to complex natural scenes, as recorded during participants’ observations [2, 16]. The dataset contains responses from eight subjects in the NSD. We use seven subjects for pretraining CLIP and Brainformer, while one is reserved for the downstream task. We follow the evaluation protocols outlined in [16], utilizing the Pearson Correlation Coefficient (PCC) score as our evaluation metric.

Performance. The results of our brain response prediction are shown in Table 2. Significantly, Brainformer yields substantial performance improvements in this task. Specifically, Swin-S/Brainformer demonstrates approximately 4.22% and 3.38% better performance than Swin-S/Random and Swin-S/CLIP, respectively. Furthermore, it is worth noting that ConvNext-based models perform strong predictive capabilities, with ConvNext-S/Brainformer achieving a PCC of 57.43%, approximately 1.73% higher than ConvNext-S/CLIP.

5. Ablation Studies

In this section, we study the efficiency of the Brain 3D Voxel Embedding as presented in Section 3.2.2, Brain fMRI Guidance Loss in Section 3.3.2, hyper-parameters of Multi-scale fMRI Transformer in Section 3.2.3, and performance of Brainformer on different amounts of data. We select ConvNext-S as the backbone for these ablation studies.

Table 1. Results of object detection and instance segmentation on COCO dataset

(a) Object Detection				
Backbone	Pretrain	AP ^{box}	AP ^{box} ₅₀	AP ^{box} ₇₅
Swin-S	Random init	41.3	63.4	45.5
Swin-S	CLIP [48]	41.9	64.0	46.0
Swin-S	Brainformer	43.6	65.8	47.4
ConvNext-S	Random init	42.6	65.5	47.0
ConvNext-S	CLIP [48]	42.8	66.1	48.3
ConvNext-S	Brainformer	45.1	68.2	50.0
(b) Semantic Segmentation				
Backbone	Pretrain	AP ^{segm}	AP ^{segm} ₅₀	AP ^{segm} ₇₅
Swin-S	Random init	38.4	60.8	41.3
Swin-S	CLIP[48]	39.2	61.3	41.7
Swin-S	Brainformer	43.1	63.1	43.3
ConvNext-S	Random init	39.8	61.7	42.9
ConvNext-S	CLIP [48]	40.8	62.2	43.5
ConvNext-S	Brainformer	44.0	64.0	45.3

Table 2. Results of semantic segmentation on ADE20K and brain activities response prediction on NSD.

Backbone	Pretrain	ADE20K mIoU	NSD PCC
Swin-S	Random init	38.37	40.41
Swin-S	CLIP [48]	40.29	41.25
Swin-S	Brainformer	41.77	44.63
ConvNext-S	Random init	39.22	54.21
ConvNext-S	CLIP [48]	41.27	55.70
ConvNext-S	Brainformer	42.92	57.43

Brain 3D Voxel Embedding. In Table 3, we provide an ablation study for 3D voxel embedding. The use of this embedding yields an improvement of approximately +3.2% box/AP, +2.2% seg/AP, +1.2% mIoU, and +1.24%PCC over the network employing traditional positional embedding in various tasks such as object detection, instance segmentation, semantic segmentation, and brain response prediction, respectively. These findings demonstrate the effectiveness of the 3D voxel embedding for fMRI signals.

Brain fMRI Guidance Loss. We also provide an ablation study for the usage of Brain fMRI Guidance Loss in Table 3. The model trained with the guidance loss performs better than not using it. In particular, this loss function helps to improve +2.4% box/AP, +3.3% seg/AP, +1.12% mIoU, and 1.18%PCC for object detection, instance segmentation, semantic segmentation, and brain response prediction, respectively. We also investigate how Brain fMRI Guidance Loss facilitates the transfer of semantic and structured information from fMRI signals to the vision model. To accomplish this, we follow a three-step process. First, we extract the fMRI features and image features from Brainformer and the vision model, respectively. Second, we compute the cosine similarity between these feature vectors. Finally, we leverage GradCam, as described in [53], by analyzing the backward gradient of the similarity to generate an attention map. This map highlights specific image regions strongly correlated to the fMRI signals. We visualize this attention map in Figure 6. It illustrates the effectiveness of the Brain fMRI Guidance Loss in transferring brain activities from the fMRI signals to the vision model.

Hyper-parameters for Multi-scale fMRI Transformer

We studied the effectiveness of the hyperparameters of Brainformer, i.e., window size and stride, on the overall performance. As shown in Table 3, the results highlight that smaller window sizes and strides lead to better performance. Increasing the window size from 64 to 128 resulted in a 2.8% decrease in box/AP, a 2.4% decrease in seg/AP, a 1.12% decrease in mIoU, and a 1.23% decrease in PCC for object detection, instance segmentation, semantic segmentation, and brain response prediction, respectively. This is attributed to the fact that a smaller window size allows Brainformer to capture more local information. Similarly, we observed similar results when keeping the window size

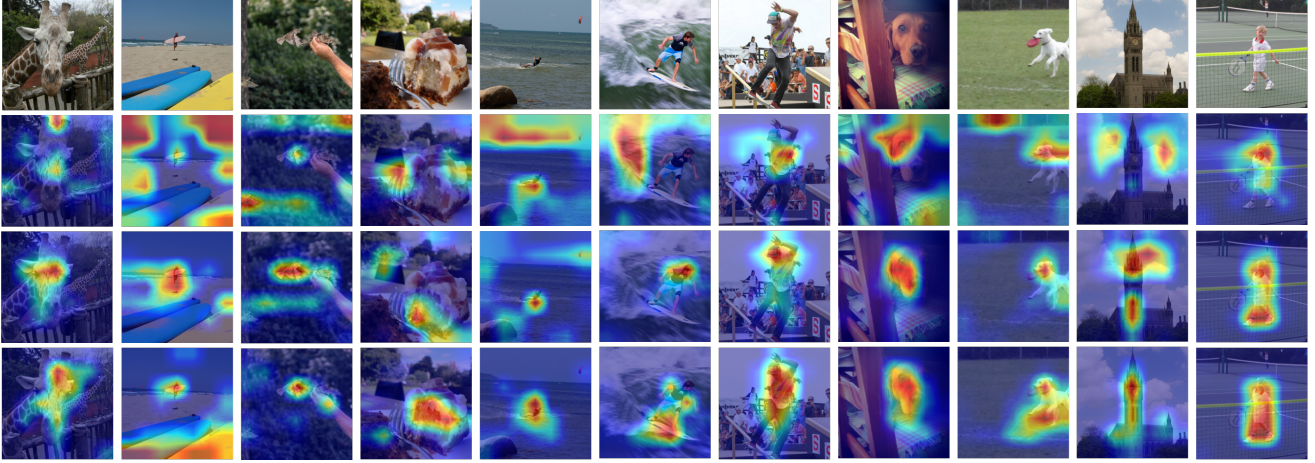


Figure 6. Visual attention with respect to fMRI signals. The first row is the input images. The second row is the corresponding attention maps of the vision model training with CLIP. The third row is the results of training with Brainformer without Brain fMRI Guidance Loss. The last row is the results with Brainformer and guidance of Brain fMRI Guidance Loss. **Best view in color.**

constant and increasing the stride from 32 to 64, with larger strides causing the model to miss more information potentially.

Performance on different amounts of data. We investigate the performance of Brainformer with respect to the amount of training data. We train the Brainformer with a different number of subjects included in the pre-training step. The performance is reported in Table 3. It is clear that when we use only one subject data, the performance is not much improved compared to the random initialization. However, when we increased the number of subjects, the performance of Brainformer also increased accordingly. With respect to 7 subjects’ training data, the performance is boosted by +2.6% for box/AP, +4.7% for seg/AP, +3.77% for mIoU, and 3.23% for PCC.

6. Conclusions and Discussions

In this paper, we have investigated the feasibility of transferring human brain activities to the vision models via fMRI signals. In our proposed Brainformer, we introduce the concept of the fMRI feature technique that explores the local patterns of the signals. Additionally, the Brain 3D Voxel

Embedding is proposed to preserve the 3D information that fMRI signals have been missed. The Multi-scale fMRI Transformer is presented to learn the features of a long signal. We also introduce Brain fMRI Guidance Loss inspired by the brain’s mechanisms to transfer the vision semantic information of humans into the vision models. The empirical experiments on various benchmarks demonstrated that Brainformer is competitive with another SOTA method that uses text modality for knowledge transfer.

Limitations and Future Works. Inspired by prior studies in neuroscience, we have developed our approach and demonstrated the efficiency of fMRI for training vision models. However, the proposed approach can potentially consist of minor limitations. First, although the NSD dataset is one of the large-scale datasets in the neuroscience field, compared to large-scale datasets such as ImageNet [12] in the computer vision field, this data is relatively small due to time and human efforts. However, we have demonstrated the performance of Brainformer with respect to the number of training data as in Section 5. The result shows that if the amount of data is sufficient, the performance of Brainformer can be better and potentially surpass the previous methods. Second, the primary goal of this study is to present a new perspective on how to involve human recognition mechanisms in training vision learning models. The experimental configurations such as utilizing CLIP [48], ConvNext [35], SwinTransformer [34] or even methods for downstream tasks, i.e., object detection, instance segmentation, semantic segmentation, and human brain response prediction, are conducted to prove our hypothesis on a fair basis. We leave further experiments with other settings for future studies.

Broader Impacts. Brainformer has a bi-directional impact on computer vision and the neuroscience field. In particular, we have illustrated how brain activities could help the vision model. Besides, Brainformer has potential benefits

Table 3. Performance of Brainformer on various settings.

	COCO		ADE20K	NSD
	AP ^{box}	AP ^{segm}	mIoU	PCC
pos embed	41.9	41.8	41.72	56.19
3D voxel embed	45.1	44.0	42.92	57.43
w/o Brain fMRI Guidance Loss	42.7	40.7	41.80	56.25
w/ Brain fMRI Guidance Loss	45.1	44.0	42.92	57.43
$w = 128, s = 64$	41.9	41.1	40.90	55.80
$w = 128, s = 32$	42.3	41.6	41.80	56.20
$w = 64, s = 32$	45.1	44.0	42.92	57.43
# subjects = 1	42.5	39.3	39.15	54.20
# subjects = 3	42.9	39.6	39.37	54.51
# subjects = 5	43.4	40.4	40.08	55.01
# subjects = 7	45.1	44.0	42.92	57.43

for neuroscientists to study brain activities, especially human cognition. Given a pair of images and corresponding fMRI, neuroscientists can utilize Brainformer as a valuable tool to explore which neurons inside the brain are highly activated with respect to the input image or particular objects inside, thus uncovering potential novel patterns of the brain.

References

- [1] Emily J Allen, Ghislain St-Yves, Yihan Wu, Jesse L Breedlove, Jacob S Prince, Logan T Dowdle, Matthias Nau, Brad Caron, Franco Pestilli, Ian Charest, et al. A massive 7t fmri dataset to bridge cognitive neuroscience and artificial intelligence. *Nature neuroscience*, 25(1):116–126, 2022. [6](#)
- [2] Emily J Allen, Ghislain St-Yves, Yihan Wu, Jesse L Breedlove, Jacob S Prince, Logan T Dowdle, Matthias Nau, Brad Caron, Franco Pestilli, Ian Charest, et al. A massive 7t fmri dataset to bridge cognitive neuroscience and artificial intelligence. *Nature neuroscience*, 25(1):116–126, 2022. [7](#)
- [3] Rajaram Anantharaman, Matthew Velazquez, and Yugyung Lee. Utilizing mask r-cnn for detection and segmentation of oral diseases. In *2018 IEEE international conference on bioinformatics and biomedicine (BIBM)*, pages 2197–2204. IEEE, 2018. [6](#)
- [4] Hangbo Bao, Li Dong, Songhao Piao, and Furu Wei. Beit: Bert pre-training of image transformers. *arXiv preprint arXiv:2106.08254*, 2021. [1](#), [2](#)
- [5] Hangbo Bao, Wenhui Wang, Li Dong, Qiang Liu, Owais Khan Mohammed, Kriti Aggarwal, Subhojit Som, Songhao Piao, and Furu Wei. Vlm: Unified vision-language pre-training with mixture-of-modality-experts. *Advances in Neural Information Processing Systems*, 35:32897–32912, 2022. [2](#)
- [6] Tom Brown, Benjamin Mann, Nick Ryder, Melanie Subbiah, Jared D Kaplan, Prafulla Dhariwal, Arvind Neelakantan, Pranav Shyam, Girish Sastry, Amanda Askell, et al. Language models are few-shot learners. *Advances in neural information processing systems*, 33:1877–1901, 2020. [1](#)
- [7] Kai Chen, Jiaqi Wang, Jiangmiao Pang, Yuhang Cao, Yu Xiong, Xiaoxiao Li, Shuyang Sun, Wansen Feng, Ziwei Liu, Jiarui Xu, Zheng Zhang, Dazhi Cheng, Chenchen Zhu, Tianheng Cheng, Qijie Zhao, Buyu Li, Xin Lu, Rui Zhu, Yue Wu, Jifeng Dai, Jingdong Wang, Jianping Shi, Wanli Ouyang, Chen Change Loy, and Dahua Lin. MMDetection: Open mmlab detection toolbox and benchmark. *arXiv preprint arXiv:1906.07155*, 2019. [6](#)
- [8] Ting Chen, Simon Kornblith, Mohammad Norouzi, and Geoffrey Hinton. A simple framework for contrastive learning of visual representations. In *International conference on machine learning*, pages 1597–1607. PMLR, 2020. [5](#)
- [9] Yen-Chun Chen, Linjie Li, Licheng Yu, Ahmed El Kholy, Faisal Ahmed, Zhe Gan, Yu Cheng, and Jingjing Liu. Uniter: Universal image-text representation learning. In *European conference on computer vision*, pages 104–120. Springer, 2020. [2](#)
- [10] Zijiao Chen, Jiaxin Qing, Tiange Xiang, Wan Lin Yue, and Juan Helen Zhou. Seeing beyond the brain: Conditional diffusion model with sparse masked modeling for vision decoding. In *Proceedings of the IEEE/CVF Conference on Computer Vision and Pattern Recognition*, pages 22710–22720, 2023. [2](#), [3](#), [4](#)
- [11] David D Cox and Robert L Savoy. Functional magnetic resonance imaging (fmri)“brain reading”: detecting and classifying distributed patterns of fmri activity in human visual cortex. *Neuroimage*, 19(2):261–270, 2003. [2](#)
- [12] Jia Deng, Wei Dong, Richard Socher, Li-Jia Li, Kai Li, and Li Fei-Fei. Imagenet: A large-scale hierarchical image database. In *2009 IEEE conference on computer vision and pattern recognition*, pages 248–255. Ieee, 2009. [1](#), [2](#), [8](#)
- [13] Jacob Devlin, Ming-Wei Chang, Kenton Lee, and Kristina Toutanova. Bert: Pre-training of deep bidirectional transformers for language understanding. *arXiv preprint arXiv:1810.04805*, 2018. [1](#), [2](#)
- [14] Alexey Dosovitskiy, Lucas Beyer, Alexander Kolesnikov, Dirk Weissenborn, Xiaohua Zhai, Thomas Unterthiner, Mostafa Dehghani, Matthias Minderer, Georg Heigold, Sylvain Gelly, et al. An image is worth 16x16 words: Transformers for image recognition at scale. *arXiv preprint arXiv:2010.11929*, 2020. [1](#)
- [15] Kshitij Dwivedi, Michael F Bonner, Radoslaw Martin Cichy, and Gemma Roig. Unveiling functions of the visual cortex using task-specific deep neural networks. *PLoS computational biology*, 17(8):e1009267, 2021. [3](#)
- [16] Alessandro T Gifford, Benjamin Lahner, Sari Saba-Sadiya, Martina G Vilas, Alex Lascelles, Aude Oliva, Kendrick Kay, Gemma Roig, and Radoslaw M Cichy. The algonauts project 2023 challenge: How the human brain makes sense of natural scenes. *arXiv preprint arXiv:2301.03198*, 2023. [6](#), [7](#)
- [17] James V Haxby, M Ida Gobbini, Maura L Furey, Almit Ishai, Jennifer L Schouten, and Pietro Pietrini. Distributed and overlapping representations of faces and objects in ventral temporal cortex. *Science*, 293(5539):2425–2430, 2001. [2](#)
- [18] John-Dylan Haynes and Geraint Rees. Predicting the orientation of invisible stimuli from activity in human primary visual cortex. *Nature neuroscience*, 8(5):686–691, 2005. [2](#)
- [19] Kaiming He, Xiangyu Zhang, Shaoqing Ren, and Jian Sun. Deep residual learning for image recognition. In *Proceedings of the IEEE conference on computer vision and pattern recognition*, pages 770–778, 2016. [1](#)
- [20] Kaiming He, Xinlei Chen, Saining Xie, Yanghao Li, Piotr Dollár, and Ross Girshick. Masked autoencoders are scalable vision learners. In *Proceedings of the IEEE/CVF conference on computer vision and pattern recognition*, pages 16000–16009, 2022. [1](#)
- [21] Gao Huang, Zhuang Liu, Laurens Van Der Maaten, and Kilian Q Weinberger. Densely connected convolutional networks. In *Proceedings of the IEEE conference on computer vision and pattern recognition*, pages 4700–4708, 2017. [1](#)
- [22] Chao Jia, Yinfei Yang, Ye Xia, Yi-Ting Chen, Zarana Parekh, Hieu Pham, Quoc Le, Yun-Hsuan Sung, Zhen Li, and Tom Duerig. Scaling up visual and vision-language representation learning with noisy text supervision. In *International conference on machine learning*, pages 4904–4916. PMLR, 2021. [2](#)

- [23] Chao Jia, Yinfei Yang, Ye Xia, Yi-Ting Chen, Zarana Parekh, Hieu Pham, Quoc Le, Yun-Hsuan Sung, Zhen Li, and Tom Duerig. Scaling up visual and vision-language representation learning with noisy text supervision. In *International conference on machine learning*, pages 4904–4916. PMLR, 2021. 1, 2
- [24] Yukiyasu Kamitani and Frank Tong. Decoding the visual and subjective contents of the human brain. *Nature neuroscience*, 8(5):679–685, 2005. 2
- [25] Nancy Kanwisher. Faces and places: of central (and peripheral) interest. *Nature neuroscience*, 4(5):455–456, 2001. 3
- [26] Peter Yongho Kim, Junbeom Kwon, Sunghwan Joo, Sangyoon Bae, Donggyu Lee, Yoonho Jung, Shinjae Yoo, Jiok Cha, and Taesup Moon. Swift: Swin 4d fmri transformer. *arXiv preprint arXiv:2307.05916*, 2023. 3
- [27] Wonjae Kim, Bokyoung Son, and Ildoo Kim. Vilt: Vision-and-language transformer without convolution or region supervision. In *International Conference on Machine Learning*, pages 5583–5594. PMLR, 2021. 2
- [28] Alex Krizhevsky, Ilya Sutskever, and Geoffrey E Hinton. Imagenet classification with deep convolutional neural networks. *Advances in neural information processing systems*, 25, 2012. 1
- [29] Mike Lewis, Yinhan Liu, Naman Goyal, Marjan Ghazvininejad, Abdelrahman Mohamed, Omer Levy, Ves Stoyanov, and Luke Zettlemoyer. Bart: Denoising sequence-to-sequence pre-training for natural language generation, translation, and comprehension. *arXiv preprint arXiv:1910.13461*, 2019. 1
- [30] Junnan Li, Dongxu Li, Caiming Xiong, and Steven Hoi. Blip: Bootstrapping language-image pre-training for unified vision-language understanding and generation. In *International Conference on Machine Learning*, pages 12888–12900. PMLR, 2022. 2
- [31] Sikun Lin, Thomas Sprague, and Ambuj K Singh. Mind reader: Reconstructing complex images from brain activities. *Advances in Neural Information Processing Systems*, 35:29624–29636, 2022. 2
- [32] Tsung-Yi Lin, Michael Maire, Serge Belongie, James Hays, Pietro Perona, Deva Ramanan, Piotr Dollár, and C Lawrence Zitnick. Microsoft coco: Common objects in context. In *Computer Vision—ECCV 2014: 13th European Conference, Zurich, Switzerland, September 6–12, 2014, Proceedings, Part V 13*, pages 740–755. Springer, 2014. 6
- [33] Yinhan Liu, Myle Ott, Naman Goyal, Jingfei Du, Mandar Joshi, Danqi Chen, Omer Levy, Mike Lewis, Luke Zettlemoyer, and Veselin Stoyanov. Roberta: A robustly optimized bert pretraining approach. *arXiv preprint arXiv:1907.11692*, 2019. 1
- [34] Ze Liu, Yutong Lin, Yue Cao, Han Hu, Yixuan Wei, Zheng Zhang, Stephen Lin, and Baining Guo. Swin transformer: Hierarchical vision transformer using shifted windows. In *Proceedings of the IEEE/CVF international conference on computer vision*, pages 10012–10022, 2021. 1, 6, 8
- [35] Zhuang Liu, Hanzi Mao, Chao-Yuan Wu, Christoph Feichtenhofer, Trevor Darrell, and Saining Xie. A convnet for the 2020s. In *Proceedings of the IEEE/CVF conference on computer vision and pattern recognition*, pages 11976–11986, 2022. 6, 8
- [36] Ilya Loshchilov and Frank Hutter. Sgdr: Stochastic gradient descent with warm restarts. *arXiv preprint arXiv:1608.03983*, 2016. 6
- [37] Ilya Loshchilov and Frank Hutter. Decoupled weight decay regularization. *arXiv preprint arXiv:1711.05101*, 2017. 6
- [38] Ziyang Luo, Pu Zhao, Can Xu, Xiubo Geng, Tao Shen, Chongyang Tao, Jing Ma, Qingwei Lin, and Daxin Jiang. Lexlip: Lexicon-bottlenecked language-image pre-training for large-scale image-text sparse retrieval. In *Proceedings of the IEEE/CVF International Conference on Computer Vision*, pages 11206–11217, 2023. 2
- [39] Dhruv Mahajan, Ross Girshick, Vignesh Ramanathan, Kaiming He, Manohar Paluri, Yixuan Li, Ashwin Bharambe, and Laurens Van Der Maaten. Exploring the limits of weakly supervised pretraining. In *Proceedings of the European conference on computer vision (ECCV)*, pages 181–196, 2018. 2
- [40] Michael C Nechyba and Yangsheng Xu. Human skill transfer: neural networks as learners and teachers. In *Proceedings 1995 IEEE/RSJ International Conference on Intelligent Robots and Systems. Human Robot Interaction and Cooperative Robots*, pages 314–319. IEEE, 1995. 2
- [41] Xuan-Bac Nguyen, Chi Nhan Duong, Xin Li, Susan Gauch, Han-Seok Seo, and Khoa Luu. Micron-bert: Bert-based facial micro-expression recognition. In *Proceedings of the IEEE/CVF Conference on Computer Vision and Pattern Recognition (CVPR)*, pages 1482–1492, 2023. 1
- [42] Satoshi Nishida, Yusuke Nakano, Antoine Blanc, Naoya Maeda, Masataka Kado, and Shinji Nishimoto. Brain-mediated transfer learning of convolutional neural networks. In *Proceedings of the AAAI Conference on Artificial Intelligence*, pages 5281–5288, 2020. 2
- [43] Furkan Ozelik and Rufin VanRullen. Brain-diffuser: Natural scene reconstruction from fmri signals using generative latent diffusion. *arXiv preprint arXiv:2303.05334*, 2023. 2
- [44] Furkan Ozelik and Rufin VanRullen. Natural scene reconstruction from fmri signals using generative latent diffusion. *Scientific Reports*, 13(1):15666, 2023. 2
- [45] Hieu Pham, Zihang Dai, Golnaz Ghiasi, Kenji Kawaguchi, Hanxiao Liu, Adams Wei Yu, Jiahui Yu, Yi-Ting Chen, Minh-Thang Luong, Yonghui Wu, et al. Combined scaling for zero-shot transfer learning. *Neurocomputing*, 555: 126658, 2023. 2
- [46] AJ Piergiovanni, Wei Li, Weicheng Kuo, Mohammad Saffar, Fred Bertsch, and Anelia Angelova. Answer-me: Multi-task open-vocabulary visual question answering. *arXiv preprint arXiv:2205.00949*, 2022. 2
- [47] William A Press, Alyssa A Brewer, Robert F Dougherty, Alex R Wade, and Brian A Wandell. Visual areas and spatial summation in human visual cortex. *Vision research*, 41 (10-11):1321–1332, 2001. 3
- [48] Alec Radford, Jong Wook Kim, Chris Hallacy, Aditya Ramesh, Gabriel Goh, Sandhini Agarwal, Girish Sastry, Amanda Askell, Pamela Mishkin, Jack Clark, et al. Learning transferable visual models from natural language supervision. In *International conference on machine learning*, pages 8748–8763. PMLR, 2021. 1, 2, 7, 8

- [49] Alec Radford, Jong Wook Kim, Chris Hallacy, Aditya Ramesh, Gabriel Goh, Sandhini Agarwal, Girish Sastry, Amanda Askell, Pamela Mishkin, Jack Clark, et al. Learning transferable visual models from natural language supervision. In *International conference on machine learning*, pages 8748–8763. PMLR, 2021. 2
- [50] Colin Raffel, Noam Shazeer, Adam Roberts, Katherine Lee, Sharan Narang, Michael Matena, Yanqi Zhou, Wei Li, and Peter J Liu. Exploring the limits of transfer learning with a unified text-to-text transformer. *The Journal of Machine Learning Research*, 21(1):5485–5551, 2020. 1
- [51] Shaoqing Ren, Kaiming He, Ross Girshick, and Jian Sun. Faster r-cnn: Towards real-time object detection with region proposal networks. *Advances in neural information processing systems*, 28, 2015. 2
- [52] Paul S Scotti, Atmadeep Banerjee, Jimmie Goode, Stepan Shabalin, Alex Nguyen, Ethan Cohen, Aidan J Dempster, Nathalie Verlinde, Elad Yundler, David Weisberg, et al. Reconstructing the mind’s eye: fmri-to-image with contrastive learning and diffusion priors. *arXiv preprint arXiv:2305.18274*, 2023. 2, 3, 4
- [53] Ramprasaath R Selvaraju, Michael Cogswell, Abhishek Das, Ramakrishna Vedantam, Devi Parikh, and Dhruv Batra. Grad-cam: Visual explanations from deep networks via gradient-based localization. In *Proceedings of the IEEE international conference on computer vision*, pages 618–626, 2017. 7
- [54] Yu Takagi and Shinji Nishimoto. High-resolution image reconstruction with latent diffusion models from human brain activity. In *Proceedings of the IEEE/CVF Conference on Computer Vision and Pattern Recognition*, pages 14453–14463, 2023. 2, 3, 4
- [55] Hao Tan and Mohit Bansal. Lxmert: Learning cross-modality encoder representations from transformers. *arXiv preprint arXiv:1908.07490*, 2019. 2
- [56] Bertrand Thirion, Edouard Duchesnay, Edward Hubbard, Jessica Dubois, Jean-Baptiste Poline, Denis Lebiha, and Stanislas Dehaene. Inverse retinotopy: inferring the visual content of images from brain activation patterns. *Neuroimage*, 33(4):1104–1116, 2006. 2
- [57] Ashish Vaswani, Noam Shazeer, Niki Parmar, Jakob Uszkoreit, Llion Jones, Aidan N Gomez, Łukasz Kaiser, and Illia Polosukhin. Attention is all you need. *Advances in neural information processing systems*, 30, 2017. 1
- [58] Peng Wang, An Yang, Rui Men, Junyang Lin, Shuai Bai, Zhikang Li, Jianxin Ma, Chang Zhou, Jingren Zhou, and Hongxia Yang. Ofa: Unifying architectures, tasks, and modalities through a simple sequence-to-sequence learning framework. In *International Conference on Machine Learning*, pages 23318–23340. PMLR, 2022. 2
- [59] Tan Wang, Kevin Lin, Linjie Li, Chung-Ching Lin, Zhengyuan Yang, Hanwang Zhang, Zicheng Liu, and Lijuan Wang. Equivariant similarity for vision-language foundation models. *arXiv preprint arXiv:2303.14465*, 2023.
- [60] Zirui Wang, Jiahui Yu, Adams Wei Yu, Zihang Dai, Yulia Tsvetkov, and Yuan Cao. Simvlm: Simple visual language model pretraining with weak supervision. *arXiv preprint arXiv:2108.10904*, 2021. 2
- [61] Tete Xiao, Yingcheng Liu, Bolei Zhou, Yuning Jiang, and Jian Sun. Unified perceptual parsing for scene understanding. In *Proceedings of the European conference on computer vision (ECCV)*, pages 418–434, 2018. 6
- [62] Zhenda Xie, Zheng Zhang, Yue Cao, Yutong Lin, Jianmin Bao, Zhuliang Yao, Qi Dai, and Han Hu. Simmim: A simple framework for masked image modeling. In *Proceedings of the IEEE/CVF Conference on Computer Vision and Pattern Recognition*, pages 9653–9663, 2022. 2
- [63] Jiahui Yu, Zirui Wang, Vijay Vasudevan, Legg Yeung, Mojtaba Seyedhosseini, and Yonghui Wu. Coca: Contrastive captioners are image-text foundation models. *arXiv preprint arXiv:2205.01917*, 2022. 2
- [64] Lu Yuan, Dongdong Chen, Yi-Ling Chen, Noel Codella, Xiyang Dai, Jianfeng Gao, Houdong Hu, Xuedong Huang, Boxin Li, Chunyuan Li, et al. Florence: A new foundation model for computer vision. *arXiv preprint arXiv:2111.11432*, 2021. 1
- [65] Xiaohua Zhai, Alexander Kolesnikov, Neil Houlsby, and Lucas Beyer. Scaling vision transformers. In *Proceedings of the IEEE/CVF Conference on Computer Vision and Pattern Recognition*, pages 12104–12113, 2022. 2
- [66] Xiaohua Zhai, Xiao Wang, Basil Mustafa, Andreas Steiner, Daniel Keysers, Alexander Kolesnikov, and Lucas Beyer. Lit: Zero-shot transfer with locked-image text tuning. In *Proceedings of the IEEE/CVF Conference on Computer Vision and Pattern Recognition*, pages 18123–18133, 2022. 2
- [67] Xiaohua Zhai, Basil Mustafa, Alexander Kolesnikov, and Lucas Beyer. Sigmoid loss for language image pre-training. *arXiv preprint arXiv:2303.15343*, 2023. 2
- [68] Pengchuan Zhang, Xiujuan Li, Xiaowei Hu, Jianwei Yang, Lei Zhang, Lijuan Wang, Yejin Choi, and Jianfeng Gao. Vinvl: Revisiting visual representations in vision-language models. In *Proceedings of the IEEE/CVF conference on computer vision and pattern recognition*, pages 5579–5588, 2021. 2
- [69] Bolei Zhou, Hang Zhao, Xavier Puig, Sanja Fidler, Adela Barriuso, and Antonio Torralba. Scene parsing through ade20k dataset. In *Proceedings of the IEEE Conference on Computer Vision and Pattern Recognition*, 2017. 6